

Simon Portegies Zwart is a Hubble Fellow

## The Evolution of Globular Clusters in the Galaxy

Koji Takahashi

Department of Earth Sciences and Astronomy,  
College of Arts and Sciences, The University of Tokyo,  
3-8-1 Komaba, Meguro-ku, Tokyo 153-8902, Japan

and

Simon F. Portegies Zwart

Department of Astronomy, Boston University,  
725 Commonwealth Avenue, Boston, MA 01581, USA

### ABSTRACT

We investigate the evolution of globular clusters using  $N$ -body calculations and anisotropic Fokker-Planck calculations. The models include a mass spectrum, mass loss due to stellar evolution, and the tidal field of the parent galaxy. Recent  $N$ -body calculations revealed a serious discrepancy between the results of  $N$ -body calculations and isotropic Fokker-Planck calculations. It has been turned out that the main reason for the discrepancy is an oversimplified treatment of the tidal field employed in the *isotropic* Fokker-Planck models. We perform a series of calculations with *anisotropic* Fokker-Planck models with a better treatment of the tidal boundary and compare these with  $N$ -body calculations. The new tidal boundary condition in our Fokker-Planck model includes one free parameter. We find that a single value of this parameter gives satisfactory agreement between the  $N$ -body and Fokker-Planck models over a wide range of initial conditions.

With this improved Fokker-Planck model we also carry out an extensive survey of the evolution of globular clusters over a wide range of initial conditions; the slope of the mass function, the central concentration and the relaxation time. The clusters are evolved up to the moment of disruption or core collapse. In general, our model clusters, calculated with the anisotropic Fokker-Planck model with the improved treatment for the tidal boundary, live considerably longer (up to an order of magnitude) than the isotropic models. The differences in the lifetime between the isotropic and anisotropic models are smallest for clusters with a steep initial mass function and with a high initial central concentration.

*Subject headings:* Galaxy: kinematics and dynamics — galaxies: kinematics and dynamics — galaxies: star clusters — globular clusters: general — open clusters and associations: general — methods: numerical

### 1. Introduction

In the last few decades Fokker-Planck models have gained in popularity for studying the dynamics of globular clusters (see Meylan & Heggie 1997 for a review). The relatively low computational cost of

Fokker-Planck models makes it possible to perform a large number of calculations over a broad range of initial parameters, and to compare the results with real observed globular clusters. The high cost of direct  $N$ -body calculations limits the choice of the number of stars to a few ten thousands, a small number compared to real globular clusters, and also limits the number of calculations which can be performed on a reasonable time scale.

Fokker-Planck calculations are relatively cheap, in terms of computer time, because of the approximations made in the method. Such approximations are absent in direct  $N$ -body models, which are therefore expected to give more reliable results than Fokker-Planck models. Our Fokker-Planck model, however, contains an extra free parameter which determines the time scale on which escaping stars leave the cluster and should be calibrated. The working hypothesis of this paper is to use the more reliable  $N$ -body calculations to calibrate this free parameter in our new Fokker-Planck model, and then to use this model to perform a series of computations to map the parameter space for the initial conditions of real globular clusters.

### 1.1. What happened before

The development of approximate methods for following the dynamical evolution of star clusters started in the 1970's using Monte-Carlo methods (Spitzer 1987, and references therein), and several groups applied these methods to address various problems in the dynamics of globular star clusters. Cohn (1979, 1980) developed a new method of solving the orbit-averaged Fokker-Planck equation directly by using a finite-difference technique. Studying the gravothermal collapse of the core of dense star clusters was popular in those days, and Cohn (1980) demonstrated that his code could follow the cluster evolution into much more advanced stages of core collapse than codes which use Monte-Carlo techniques to solve the equations of motion of the stars (see, however, Giersz 1998, for a possible revival of the Monte-Carlo methods).

Cohn (1979, 1980) modeled globular clusters as fairly idealized systems, i.e.: isolated systems of identical point masses. This was quite a natural starting point for theoretical studies. After Cohn's seminal works, many contributions have made improvements to Fokker-Planck models in terms of adding various astrophysical processes, such as: a mass spectrum, primordial binaries, a tidal cut-off, gravitational shocks by the galactic disk and the bulge, mass loss from stellar evolution, the anisotropy of the velocity distribution, initial rotation of the clusters, etc. (see Meylan & Heggie 1997, for a review).

An important landmark in modeling the evolution of globular clusters with Fokker-Planck calculations was set by Chernoff & Weinberg (1990, hereafter CW). The models of CW included a tidal cut-off of the parent galaxy, a stellar mass spectrum and mass loss due to stellar evolution. According to Meylan & Heggie (1997), CW is an excellent starting point for learning what the Fokker-Planck model can teach us about the evolution of model star clusters.

CW boldly added simultaneously several new astrophysical phenomena to their models. However, each time a model is extended in order to add more realism to the calculations, the number of assumptions increases and thorough testing is required (not only for Fokker-Planck models) to eliminate the possible introduction of omissions. In addition it should be tested whether the improvements do not interfere with some of the earlier assumptions on which the integration technique is based, and whether the new model can follow the evolution of the star cluster still reliably. Of course it is hard to prove the reliability of a model, but comparison between two completely different techniques may be one of the most convenient and reliable ways to obtain an indication of the realism of both methods.

Such comparisons have found good agreements between  $N$ -body, Fokker-Planck and gaseous models for isolated globular clusters of point masses (Giersz and Heggie 1994a, 1994b; Giersz and Spurzem 1994; Spurzem and Takahashi 1995). These are important results because they demonstrate that two-body relaxation, which is expected to drive the dynamical evolution of star clusters, is indeed dominant. It also shows that the time evolution of such relatively simple star clusters scales, as expected, with the two-body relaxation time.

Fukushige & Heggie (1995) and Portegies Zwart et al. (1998), however, demonstrated that  $N$ -body calculations, which include the steady tidal field of the parent galaxy and mass loss due to stellar evolution, gave completely different results than the Fokker-Planck calculations of CW. The results of the computations of Portegies Zwart et al. (1998) can be summarized as follows: 1) The  $N$ -body model with the largest number of particles has a life time more than an order of magnitude longer than that of the comparable isotropic Fokker-Planck calculation. 2) The life time of the cluster depends on the number of stars in a rather complex way.

Takahashi & Portegies Zwart (1998, TPZ hereafter) solved these discrepancies by using anisotropic Fokker-Planck models together with an improved treatment of the tidal boundary. Their calculations took account of the dependence of the escape condition on the orbital angular momentum (Takahashi et al. 1997) and the time scale on which these escaping stars physically leave the cluster (Lee & Ostriker 1987). With these improvements they achieved excellent agreement between  $N$ -body and Fokker-Planck calculations. It turned out that the assumption of velocity isotropy and the oversimplified escape condition adopted by CW resulted in an enormous over estimate of the escape rate, i.e.: an under estimate of the life time. A star on an escaping orbit requires about a crossing time at the tidal radius to leave the cluster. The number of stars that escape per relaxation time depends therefore on the ratio of the relaxation time to the dynamical time, i.e.: on the number of stars.

TPZ's implementation of the escape condition adds a free parameter  $\nu_{\text{esc}}$  (denoted by  $\alpha_{\text{esc}}$  in TPZ) to the models. This parameter determines the time scale on which escaping stars leave the cluster, and should be of the order of the crossing time at the tidal radius (Lee & Ostriker 1987; see also Ross et al. 1997). TPZ calibrated  $\nu_{\text{esc}}$  on one specific set of initial conditions: density profile, mass function and relaxation time. However, it is not at all obvious that a single value of  $\nu_{\text{esc}}$  gives good agreements between Fokker-Planck and  $N$ -body calculations for a wide range of initial conditions. The major goal of this paper is to test this hypothesis.

The second purpose of this paper is to carry out an extensive survey of initial conditions to the evolution of globular clusters in the galaxy. We use the improved anisotropic Fokker-Planck models to perform such a survey and we use the initial conditions set out in the survey performed by CW.

In the following section we review the anisotropic Fokker-Planck model and the  $N$ -body model. In section 3 the stellar evolution models are described and the initial conditions are reviewed in section 4. The results of our calculations are presented in section 5. The results are discussed in section 6 and they are summarized in the last section.

## 2. The Models

## 2.1. The Fokker-Planck model

We use anisotropic orbit-averaged Fokker-Planck models (Cohn 1979; Takahashi 1995). The star clusters are assumed to be spherically symmetric and in dynamical equilibrium, at any time. The distribution function  $f$  at time  $t$  is then a function of the energy of a star per unit mass,  $E$ , and the angular momentum per unit mass,  $J$  (see e.g.: Spitzer 1987, section 1.2). We do not a priori assume that the velocity distribution is isotropic, i.e.: the radial velocity dispersion and the (one-dimensional) tangential velocity dispersion are allowed to differ. We therefore call these models: *anisotropic* Fokker-Planck models. In *isotropic* Fokker-Planck models (Cohn 1980), on the other hand, the velocity distribution is assumed to be isotropic and the distribution function  $f$  depends only on the energy.

Anisotropic Fokker-Planck models are more general than isotropic Fokker-Planck models and therefore also preferable. The higher computational costs and more complex numerical implementation, however, caused anisotropic Fokker-Planck models to be less favored than their isotropic cousins (Cohn 1980). But the numerical problem which were encountered by Cohn (1979) in the anisotropic Fokker-Planck models were solved by Takahashi (1995; 1996) by implementing a new finite-difference scheme (see also Drukier et al. 1999).

All Fokker-Planck calculations in this paper are performed with the code developed by Takahashi (1995; 1996). It was later modified to include a mass function for single stars (Takahashi 1997), a tidal boundary (Takahashi et al. 1997; TPZ), and stellar evolution (TPZ).

### 2.1.1. Determination of escaping stars

TPZ demonstrated that the results of Fokker-Planck calculations are sensitive to the choice of the tidal boundary conditions. Two different criteria for the identification of escapers were tested by Takahashi et al. (1997) and TPZ. These are 1.) the apocenter criterion, in which a star is removed if

$$r_a(E, J) > r_t, \quad (1)$$

and 2.) the energy criterion, in which a star is removed if

$$E > E_t \equiv -GM/r_t. \quad (2)$$

Here  $r_a(E, J)$  is the apocenter distance of a star with energy  $E$  and angular momentum  $J$ ,  $M$  is the mass of the cluster and  $r_t$  is its tidal radius.

The apocenter criterion is considered more realistic than the energy criterion. The latter tends to removes to many stars; it sometimes even removes stars with orbits inside the tidal radius. For the calculations performed in this paper we adopt the apocenter criterion to determine the escapers for our Anisotropic Fokker-Planck models. We call such models “Aa models” (see TPZ).

### 2.1.2. Introducing the crossing time in the Fokker-Planck model

In the Fokker-Planck calculations performed by CW, escapers are removed instantaneously from the modeled clusters. In the absence of stellar evolution this condition may be justified if the dynamical time scale of the cluster is negligible compared to the two-body relaxation time, e.g.: if the number of stars  $N \rightarrow \infty$  with a constant relaxation time.

In practice an escaping star does not leave the cluster instantaneously. TPZ demonstrated that the lifetime of the stellar system with small  $N$  is dramatically affected by the time scale on which escaping stars are removed from the stellar system. Two treatments for escaping stars were tested by TPZ; 1.) instantaneous escape: a star is removed from the cluster as soon as it satisfies an adopted escape criterion, and 2.) crossing-time escape: a star hangs around in the cluster for a certain time before it is removed.

To implement the crossing-time escape condition in Fokker-Planck calculations, we use the following boundary condition (Lee & Ostriker 1987):

$$\frac{df}{dt} = -\nu_{\text{esc}} f \left[ 1 - \left| \frac{E}{E_t} \right|^3 \right]^{1/2} \frac{1}{2\pi} \sqrt{\frac{4\pi}{3} G \rho_t}. \quad (3)$$

Here  $\rho_t$  is the mean mass density within the tidal radius and  $\nu_{\text{esc}}$  is a dimensionless constant which determines how quickly escapers leave the cluster. This equation is applied in the region where the adopted escape criterion is satisfied in  $(E, J)$ -space. Eq. (3) is derived assuming that escapers leave the cluster on a dynamical time scale. For  $N \rightarrow \infty$ , this condition becomes identical to removing escapers instantaneously since the ratio of the crossing time to the relaxation time vanishes.

For the models which use equation (3) the density at the tidal radius is generally still finite. The total mass for these cluster is that within the tidal radius  $r_t$ .

### 2.1.3. The mass function

In our Fokker-Planck models a continuous mass function is represented by  $K$  discrete mass components. We use  $K = 20$  for all Fokker-Planck calculations. At  $t = 0$  the mass of a star in mass-bin  $k$  is given by

$$m_k = m_- \left( \frac{m_+}{m_-} \right)^{(k-\frac{1}{2})/K}. \quad (4)$$

Here  $m_-$  and  $m_+$  are the lower and upper limits of the initial mass function. The total mass in mass interval  $k$  is

$$M_k = \int_{m_{k-\frac{1}{2}}}^{m_{k+\frac{1}{2}}} \frac{dN}{dm} m dm. \quad (5)$$

Here  $dN/dm$  is the number of stars per unit mass interval.

## 2.2. The $N$ -body model

The  $N$ -body portion of the simulations is carried out using the **Kira** integrator, operating within the Starlab (version 3.3) software environment (McMillan & Hut 1996; Portegies Zwart et al. 1998). Time integration of stellar orbits is accomplished using a fourth-order Hermite scheme (Makino & Aarseth 1992). **Kira** also incorporates block time steps (McMillan 1986a; 1986b; Makino 1991), special treatment of close two-body and multiple encounters of arbitrary complexity, and a robust treatment of stellar and binary evolution and stellar collisions (Portegies Zwart et al. 1999). The special-purpose GRAPE-4 (Makino et al. 1997) system is used to accelerate the computation of gravitational forces between stars. The treatment of stellar mass loss is described in Portegies Zwart et al. (1998). A more complete description of the Starlab environment is in preparation but more information can be found at the following URL <http://www.ias.edu/~starlab>.

### 3. Stellar Evolution

#### 3.1. *N*-body Models

Stars in the *N*-body calculations are evolved with the stellar evolution model **SeBa**<sup>1</sup> (Portegies Zwart & Verbunt 1996, Section 2.1). In **SeBa** stars with a mass between  $8 M_{\odot}$  and  $15 M_{\odot}$  become neutron stars with  $m_{\text{fin}} = 1.34 M_{\odot}$  and stars with  $m < 8 M_{\odot}$  become white dwarfs. The mass of these white dwarfs are given by the core mass of their progenitors. For the Fokker-Planck models this is extrapolated from a tabulated data as listed in Table 1.

The evolution of the stars in the Fokker-Planck calculations which are compared with the *N*-body runs are also computed using **SeBa**.

#### 3.2. Fokker-Planck models

We use the same stellar evolution model as was adopted by CW when we attempt to compare our anisotropic Fokker-Planck models with their results. The stars in this model live somewhat shorter than those in **SeBa** (see Table 1).

Table 1 compares the stellar evolution model used by CW with **SeBa**. The main-sequence lifetime of the CW model is obtained by fitting cubic splines to the data listed in Table 1 of CW. The lowest mass in the table provided by CW is  $m \simeq 0.83 M_{\odot}$ . They did not explain how to extrapolate the stellar lifetimes to lower masses. Since some clusters become considerably older than 15 Gyr, it is necessary to use proper lifetimes for these stars. The lifetimes for stars with  $m < 0.83 M_{\odot}$  are computed by assuming the following dependence  $m^{-3.5}$  (Drukier 1995). This power law also gives a good fit to the lifetimes of the low-mass stars in **SeBa** (see Table 1).

At the end of its lifetime, a star with an initial mass  $m_{\text{ini}}$  forms a compact object with mass  $m_{\text{fin}}$ . In the model adopted by CW the mass or the remnant is given by

$$m_{\text{fin}} = \begin{cases} 0.58 + 0.22(m_{\text{ini}} - 1), & \text{for } m_{\text{ini}} < 4.7 [M_{\odot}], \\ 0, & \text{for } 4.7 \leq m_{\text{ini}} \leq 8.0 [M_{\odot}], \\ 1.4, & \text{for } 8.0 < m_{\text{ini}} \leq 15.0 [M_{\odot}]. \end{cases} \quad (6)$$

Stars with mass  $m_{\text{ini}} \lesssim 0.46 M_{\odot}$  do not lose any mass in a stellar wind and turn into white dwarfs at the end of their lifetime.

The mass of the  $k$ -th component is decreased from its initial mass  $m_k^{\text{ini}}$  to the final (remnant) mass  $m_k^{\text{fin}}$  linearly in time  $t$  during the period of  $t_{\text{MS}}(m_{k+1/2}^{\text{ini}}) < t < t_{\text{MS}}(m_{k-1/2}^{\text{ini}})$ , where  $t_{\text{MS}}(m)$  is the main-sequence lifetime of a star with the initial mass  $m$ .

### 4. Initial Conditions

The initial conditions for our Fokker-Planck calculations are identical to those of the survey performed by CW. The galaxy is assumed to be spherical and the star clusters are on circular orbits around the

---

<sup>1</sup>The name **SeBa** is adopted from the Egyptian word for ‘to teach’, ‘the door to knowledge’ or ‘(multiple) star’. The exact meaning depends on the hieroglyphic spelling.

galactic center. The tidal radius changes with time as  $r_t(t) \propto M^{1/3}(t)$ . The initial density profiles of the star clusters are set up from King models (King 1966). The dimensionless central potential of these King models is chosen from  $W_\circ = 1, 3$  and  $7$ . The initial mass function is given by

$$dN \propto m^{-\alpha} dm, \quad (7)$$

with  $\alpha = 1.5, 2.5$  and  $3.5$  between  $m = 0.4 M_\odot$  and  $15 M_\odot$ .

In addition to the two dimensionless parameters  $W_\circ$  and  $\alpha$ , there is, apart from the number of stars, one more free parameter: the initial relaxation time, which CW defined as follows;

$$t_{\text{rlx}} = 2.57 F \text{ [Myr]}, \quad (8)$$

where

$$F \equiv \frac{M}{M_\odot} \frac{R_g}{\text{kpc}} \frac{220 \text{ km s}^{-1}}{v_g} \frac{1}{\ln N}. \quad (9)$$

Here  $M$  is the total mass of the cluster,  $R_g$  is its distance to the Galactic center,  $v_g$  is the circular speed of the cluster, and  $N$  is the total number of stars. (This expression for the relaxation time is derived from CW's equations [1], [2], and [6] with  $m = M_\odot$ ,  $r = r_t$ , and  $c_1 = 1$ .)

Following CW, a group of models with the same  $F$  (constant relaxation time) at the start of the simulation is referred to as a family. Our survey covers CW's families 1, 2, 3 and 4. Table 2 reviews the properties of the selected families. For convenience Table 2 also gives the relaxation time at the half-mass radius  $t_{\text{rh}}$  for the models with  $W_\circ = 3$  and  $\alpha = 2.5$  (mean stellar mass  $\bar{m} \simeq 1 M_\odot$ ), which we compute with (Spitzer 1987, p. 40)

$$t_{\text{rh}} = 0.138 \frac{N^{1/2} r_{\text{h}}^{3/2}}{\bar{m}^{1/2} G^{1/2} \ln N}. \quad (10)$$

Here  $r_{\text{h}}$  is the half-mass radius.

We perform the same survey in initial conditions as CW. They assumed that the evolution of clusters is completely determined by the three parameters:  $W_\circ$ ,  $\alpha$ , and  $F$ . However, Portegies Zwart et al. (1998) demonstrated that the evolution of a star cluster also depends on the number of stars! This dependence is introduced in our anisotropic Fokker-Planck calculations by equation (3), which contains the free parameter  $\nu_{\text{esc}}$  (TPZ).

In the following § we compare the results of the performed  $N$ -body calculations with our anisotropic Fokker-Planck calculations. The escaping stars in our Fokker-Planck models are removed on the appropriate time scale, using Eq. (3) with the selected  $\nu_{\text{esc}}$ . To test the effect of increasing the number of stars on the results we also perform a number of Fokker-Planck calculations with  $N = 3 \times 10^5$  (also using Eq. [3] and the same  $\nu_{\text{esc}}$ ) and, for CW's entire survey in parameter space, with the anisotropic Fokker-Planck model with the instantaneous escape condition. (The latter choice eliminates the freedom in  $\nu_{\text{esc}}$  since the condition of equation (3) approaches the instantaneous escape condition for  $N \rightarrow \infty$ .)

## 5. Results

### 5.1. Comparison between Fokker-Planck and $N$ -body Models

### 5.1.1. The time evolution of the total mass

TPZ performed a series of calculations with Fokker-Planck models and  $N$ -body models (with  $N=1K$  to  $32K$ ,  $K\equiv 1024$ ) for one set of initial conditions ( $W_0 = 3$ ,  $\alpha = 2.5$ , family 1). The agreement between their anisotropic Fokker-Planck models ( $Aa$  models with eq. [3]) and the  $N$ -body models is excellent. Figure 1 reproduces their main results on which they calibrated  $\nu_{\text{esc}}$  (see eq. [3]). However, note  $\nu_{\text{esc}} = 2.5$  is used in the Fokker-Planck calculations shown in this figure, but  $\nu_{\text{esc}} = 2$  in TPZ’s calculations.

To test whether a single value of  $\nu_{\text{esc}}$  gives satisfactory agreement between Fokker-Planck and  $N$ -body calculations over a wide range of initial conditions, we performed a number of calculations with various  $N$  and various initial conditions to search for the optimal value of  $\nu_{\text{esc}}$ . This calibration of  $\nu_{\text{esc}}$  is rather subtle because a perfect agreement between the Fokker-Planck models and the  $N$ -body models is not obtained with any value of  $\nu_{\text{esc}}$  and due to different statistical characteristics of both models (see TPZ). We conclude that  $\nu_{\text{esc}} = 2.5$  gives the best agreement over the entire range of initial conditions. This value is slightly larger than the  $\nu_{\text{esc}} = 2.0$  which was used by TPZ.

We perform  $N$ -body and Fokker-Planck calculations with initially  $8K$  and  $16K$  stars for each selected set of initial conditions (for economical reasons one set of initial conditions is computed with only  $4K$  and  $8K$  stars). One extra Fokker-Planck calculation for each set of initial conditions is performed with the instantaneous escape condition ( $N \rightarrow \infty$ ) to compare the result with real globular clusters.

Figures 2 to 6 present the evolution of the total mass of the clusters calculated with the  $N$ -body model as well as with the Fokker-Planck model. The same value of  $\nu_{\text{esc}} = 2.5$  is used for all Fokker-Planck calculations. The agreement between Fokker-Planck and  $N$ -body calculations is excellent over the entire range of initial conditions. Apparently a single value of  $\nu_{\text{esc}}$  is applicable.

Figure 4 gives the results for  $W_0 = 3$ ,  $\alpha = 2.5$ , family 4, which shows a clear difference between Fokker-Planck and  $N$ -body results. The  $N$ -body models tend to lose their mass more quickly than the appropriate Fokker-Planck models. The mass loss in the  $N$ -body models accelerates compared with the Fokker-Planck models (from about 1 Gyr for the  $16K$  model and from about 2 Gyr for the  $8K$  model), and after some time it becomes slower again. The same behavior is also observable in the other models and in the calculations performed by TPZ (see Fig. 1). This phased mass loss is a retardation effect in the  $N$ -body models of the coupling between the mass lost by stellar evolution and the removal of escaping stars. We discuss this behavior in more detail in § 6.4.

Figure 5 shows the evolution of a model in which the initial mass function is rather flat and with a deep central potential ( $W_0 = 7$ ,  $\alpha = 1.5$ , family 4). The evolution of the total mass of this cluster is peculiar; it loses about 80% of its mass within the first billion years. Mass loss in this cluster is mainly driven by stellar evolution. The flat initial mass function causes about 33% (in mass fraction) of the stars to leave the main sequence within 1 Gyr. The fraction of mass lost by the cluster due to stellar evolution alone is therefore about 62%. Nevertheless the cluster still survives beyond 10 Gyr. The high central concentration ( $W_0 = 7$ ) is the main reason why this cluster is not dissociated due to the excessive mass loss. In the first 1 Gyr the halo of the cluster is stripped almost completely, but the compact core survives. Even in this extreme case the agreement between Fokker-Planck and  $N$ -body models is good. However, a similar behavior as in Fig. 4 is visible in sense that in the first Gyr the  $N$ -body models lose mass slightly more quickly than the Fokker-Planck models.

### 5.1.2. The mass function at $t = 10$ Gyr

At the start of each calculation the Fokker-Planck model and the  $N$ -body model have the same mass function. This mass function is the same throughout the entire cluster. Mass loss by stellar evolution and mass segregation due to the dynamical evolution of the star cluster cause the global mass function as well as the local mass function to change in time. After some time the mass function becomes clearly a function of the distance to the cluster center.

Figure 7 shows the mass function for the  $N$ -body and the Fokker-Planck calculations for the model with  $W_0 = 7$ ,  $\alpha = 2.5$  and family 1 at an age of 10 Gyr. At that moment the clusters have lost approximately 60% of their initial mass (see Fig. 3). The differences between the global mass-functions of the  $N$ -body model and of the Fokker-Planck model are negligible. Even the partial mass functions for the main-sequence stars and for the compact objects (white dwarfs and neutron stars) agree excellently. At an age of 10 Gyr the mass function for the main-sequence stars is somewhat flatter than the initial mass function. The shape of the mass function, however, is still well represented by a single power-law. We compared the mass functions between Fokker-Planck and  $N$ -body models at  $t = 10$  Gyr for several other cases also, and in all these cases the agreement was good.

## 5.2. Fokker-Planck Survey Results

In this § we present the results of our anisotropic Fokker-Planck calculations in which escaping stars are removed instantaneously from the cluster. These calculations give lower limits to the lifetimes of the clusters (see TPZ).

Table 3 summarizes the survey results and compares them with the results obtained by CW (their Table 5). Following CW, the fate of the cluster is classified as ‘C’ for core collapse or ‘D’ for disruption. The mass of the cluster (in units of the initial mass) and the time (in Gyrs) at the moment we stop the calculations (resulting in C or D) are listed in Table 3. The end time for clusters which experience core collapse indicates the moment that the collapse occurs. These clusters may well survive beyond this time but their evolution is not followed any further.

By definition a cluster ceases to exist (is disrupted) at the moment  $M = 0$ . The exact moment at which this happens is not easily determined in the Fokker-Planck calculations. Mass loss often accelerates before the moment the cluster evaporates (see Figure 8). In such a case the Fokker-Planck model fails to find a self-consistent solution for the potential, and breaks. The moment this happens may be associated with the moment equilibrium is lost by the cluster (Fukushige & Heggie 1995). This makes it hard to identify the exact moment of disruption, and we therefore adopt the moment that the mass loss rate becomes virtually infinite as the disruption time. The mass of the cluster at this point is given in Table 3.

### 5.2.1. The time evolution of the total mass and the concentration parameter

Figure 8 shows the evolution of the total mass for all models. The circles plotted at the ends of some of the lines indicate the moments that these clusters experience core collapse. The mass evolution, the lifetime and the fate of the modeled clusters are determined by the selected initial conditions ( $W_0$ ,  $\alpha$  and family). The early evolution is generally strongly affected by the choice of  $W_0$  and  $\alpha$  and in less extent by the initial relaxation time, simply because the latter requires more time to affect the dynamics

of the stellar system. The lifetimes of the clusters which are disrupted within  $\sim 1$  Gyr, for example, are almost independent of the initial relaxation time. The evolution of these clusters is mainly driven by stellar mass loss which causes the clusters to expand homologously. Core collapse occurs only in some long-lived ( $t > 3$  Gyr) clusters. For these models the mass loss rate gradually decreases with time (see also Portegies Zwart et al. 1998).

Figure 9 shows the evolution of the concentration parameter  $c$ , which we define by

$$c \equiv \log_{10} \frac{r_t}{r_c}. \quad (11)$$

Here the core radius  $r_c$  is

$$r_c = \left( \frac{3v_{m0}^2}{4\pi G \rho_0} \right)^{1/2} \quad (12)$$

with  $\rho_0$  as the central density and  $v_{m0}$  is the density-weighted velocity dispersion in the cluster center. The definitions of the core radius (12) and the concentration (11) come from King's (1966) definitions. (Note that this core radius  $r_c$  and the King radius are not identical even for a single-mass system, since the central velocity dispersion is not used in the definition for the King radius. The two definitions approach each other for more concentrated [higher  $W_\circ$ ] clusters [cf. Binney & Tremaine 1987, p. 235].)

In some cases (for  $W_\circ = 7$ ,  $\alpha = 1.5$ , families 1 to 4 and for  $W_\circ = 1$ ,  $\alpha = 3.5$ , family 1) the cluster experiences core collapse after almost all the mass ( $\gtrsim 99\%$ ) is lost. These clusters are regarded as collapsed clusters, because the concentration  $c$  rapidly increases at the final epochs (see Figure 9). If the initial mass of a cluster is relatively small (e.g.  $M \lesssim 10^4 M_\odot$ ), deep core collapse may be prevented by the presence of three-body binary heating. Such effects are not taken account of in our Fokker-Planck models.

All clusters with families 2, 3 and 4 for  $W_\circ = 7$  and  $\alpha = 1.5$  have very small masses (compared to their initial masses) around  $t = 10$  Gyr. This implies that these clusters may at present be observed as tiny globular clusters or as old open clusters (see § 6.3). For all models with  $\alpha = 1.5$  mass loss due to stellar evolution causes the concentration to decrease in time before core collapse occurs. For  $\alpha = 2.5$  and 3.5 the concentration does not decrease so much but stays almost constant in time. If, at any time, the concentration becomes smaller than  $c \approx 0.4$  the cluster quickly dissolves.

### 5.2.2. Comparison with Chernoff & Weinberg (1990)

Table 3 compares the results of CW with our  $Aa$  models. All our calculated clusters disrupt later than those of CW. In some cases ( $W_\circ = 1$ ,  $\alpha = 2.5$  and family 3) the discrepancy in the lifetime exceeds a factor of ten. The discrepancy in the lifetime of the clusters with  $\alpha = 1.5$  and  $W_\circ = 1$  and those with  $W_\circ = 3$  is only a factor of two. These models disrupt very quickly and the introduction of the anisotropy does not extend their lifetimes very much because the combination of a flat initial mass function and a shallow initial potential causes the cluster to lose mass so quickly that there is hardly time for an anisotropy to develop.

About half (17) of the clusters calculated with anisotropic models experience core collapse, where in the calculations of CW less than 30% (10) of the clusters experience core collapse. This means that seven of the models for which CW predicts disruption experience core collapse according to our calculations. The collapse of these models occurs much later than that CW's clusters are disrupted; the high rate of mass loss causes their clusters to disrupt too quickly.

All the clusters which experience core collapse according to CW also experience core collapse in our

calculations. Core collapse occurs when the time scale on which the cluster loses mass is much longer than the relaxation time. Therefore it is not surprising that for these clusters CW's results and our results show a smaller discrepancy. In particular for the initial models with a deep potential well ( $W_0 = 7$ ) and a relatively steep mass function ( $\alpha = 2.5, 3.5$ ) the difference in collapse time between our models and CW models is only  $O(10)\%$ .

Figure 10 gives a graphical representation of table 3 for family 1. The largest discrepancies occur for relatively shallow potential models with short lifetimes.

### 5.3. Fokker-Planck Survey Results: $N = 3 \times 10^5$

The evolution of a cluster depends on the number of stars  $N$  as well as on  $W_0$ ,  $\alpha$ , and the initial relaxation time (see TPZ and § 5.1). We presented in § 5.2 the results of calculations where we use the instantaneous removal of escapers, i.e.:  $N \rightarrow \infty$ . The removal condition based on the crossing time is used in the calculations shown in § 5.1, for relatively small  $N$  clusters. In this § show the results of a series of calculations for which  $N$  is chosen to be small but large enough to represent the number of stars in a small globular cluster.

Figure 11 presents the mass evolution of models of family 4 with  $N = 3 \times 10^5$  at the initial time; the initial total masses are  $7.3 \times 10^5 M_\odot$ ,  $3.0 \times 10^5 M_\odot$ , and  $2.0 \times 10^5 M_\odot$  for  $\alpha = 1.5, 2.5$ , and  $3.5$ , respectively. These are compared with the models with  $N \rightarrow \infty$  (presented also in Fig. 8). Since family 4 has the largest relaxation time of all families it also has the largest crossing time which makes these models most susceptible to the crossing time removal condition. The difference between the models with  $N = 3 \times 10^5$  and those with  $N \rightarrow \infty$  is strongest for clusters which disrupt relatively quickly, within 10 Gyr. In these cases the models with  $N = 3 \times 10^5$  live a factor of two or three longer than those models with the instantaneous escape condition. We therefore conclude that for rich globular clusters which have survived for a Hubble Time the instantaneous removal condition gives good results.

## 6. Discussion

### 6.1. The Anisotropic Fokker-Planck Model

Our anisotropic Fokker-Planck models are in excellent agreement with  $N$ -body models for a wide range of initial conditions. Although it was to be expected from theoretical considerations, we find it still quite striking that a single value of  $\nu_{\text{esc}}$  suffices to achieve agreement between the very different types of models and over such a wide range in initial conditions. Subtle differences between the Fokker-Planck and the  $N$ -body results, however, remain. These are mainly a result of the greater detail and higher accuracy of the  $N$ -body models compared to the Fokker-Planck calculations and by the relatively simplistic implementation of the tidal field via a cut-off radius (see § 6.4).

The differences between our anisotropic Fokker-Planck calculations and the isotropic Fokker-Planck calculations of CW are very significant. The anisotropic Fokker-Planck models live considerably longer than the isotropic models. The discrepancy is mainly caused by the different implementations of the boundary conditions (see § 2.1), i.e.: the way escaping stars are removed. Mass loss from the cluster is crucial for its survival under the influence of stellar evolution and the tidal field of a parent galaxy. The apocenter criterion is considered more realistic than the energy criterion, but the implementation of the apocenter

criterion requires anisotropic Fokker-Planck models. Isotropic Fokker-Planck models can only use the energy criterion and therefore results in too short cluster lifetimes.

The mass-loss rate of a cluster depends on the angular-momentum distribution of the stars near the tidal boundary. This velocity anisotropy depends on the masses of the stars and on their distance to the cluster center, which change in time in a complicated way. Therefore there seems to be no trivial way at which isotropic Fokker-Planck models can be modified in order to make them reproduce the results of anisotropic Fokker-Planck models.

### 6.2. Comparison with Aarseth & Heggie (1998)

Recently Aarseth & Heggie (1998) performed  $N$ -body calculations of star clusters in order to investigate the time scaling of  $N$ -body models with respect to the number of stars. They incorporate the tidal field of the parent galaxy in a similar fashion as in the simulations of Fukushige & Heggie (1995). Stellar evolution is implemented in the same fashion as is done by Portegies Zwart et al. (1998), and in the present study.

Aarseth & Heggie (1998) have a different approach for scaling cluster evolution with respect to the number of stars. To obtain a better comparison between their  $N$ -body calculations and the Fokker-Planck results of CW, Aarseth & Heggie (1998) introduce a new variable time scaling for the stellar evolution in the  $N$ -body calculations. Their scaling is a hybrid of two fixed time scalings: the crossing-time scaling and the relaxation-time scaling. They use the crossing-time for the time scaling during the phase in which the clusters' mass loss is driven by stellar evolution. When two-body relaxation becomes important they use the clusters' relaxation-time to scale. This variable time scaling has a qualitative physical basis, but the uncertainties in when and how to switch from one scaling to the other are considerable.

Using this hybrid time scaling Aarseth & Heggie (1998) find good agreement between their  $N$ -body calculations and the Fokker-Planck calculations of CW for clusters that survive long enough for their evolution to become dominated by two-body relaxation. According to their calculations the quickly disrupting clusters of CW live too short compared to their simulations. These conclusions are qualitatively consistent with our findings. A more detailed comparison between Aarseth & Heggie's (1998)  $N$ -body calculations and our Fokker-Planck calculations is complicated by the difference in the implementation of the tidal field; they use a self-consistent tidal field.

### 6.3. Comparison with the observations

Comparing our results with observed globular clusters is not easy. The main goal of this paper was to review the results obtained by CW and the initial conditions they selected are possibly not the best choice for real globular clusters. Deep surveys have revealed that the mass function is ill represented by a single power-law (Scalo 1986, Kroupa et al. 1990) and the adopted lower mass limit of  $0.4 M_{\odot}$  is too high (De Marchi & Paresce 1995a; 1995b; Marconi et al. 1998; see also Chernoff 1993). Another uncertainty, which may seriously affect the results, is the initial compactness of the star clusters relative to their tidal radius. We assumed that at the start of the calculations the tidal radius equals the truncation radius of the King model (i.e. the radius beyond which the density vanishes). King models, however, are not the best choice for the initial density profiles for tidally-truncated star clusters (Heggie & Ramamani 1995). It is not even clear whether real globular clusters are born filling up their tidal lobes. If clusters are born well inside their

Roche-lobes, their lifetime is extended substantially.

Regardless of the uncertainties in the initial conditions, we like to discuss some of the consequences for the observed population of globular clusters. In that respect our calculations indicate that clusters which are observed in a state of core collapse must have started fairly concentrated; otherwise these clusters would not reach core collapse within the age of the Universe. At the moment core collapse is reached these clusters generally have lost  $\gtrsim 50\%$  of their mass. This indicates that observed globular clusters in a state of core collapse were born rather concentrated and considerably more massive than what is observed.

All the clusters with a concentration parameter  $c \simeq 1$  at  $T \simeq 10$  Gyr appear to be in a local minimum in concentration. These clusters recover later as they experience core collapse. Our results indicate that each cluster which reaches a concentration of  $c \simeq 0.5$  at some instant evaporates quickly thereafter. On the other hand, the least concentrated globular clusters in our Galaxy have a King concentration parameter of  $c_{\text{King}} \simeq 0.5$  (Trager et al. 1993). This is consistent with our findings.<sup>2</sup>

It is interesting to search for relics of those clusters whose initial conditions are characterized by  $W_0 = 7$  and  $\alpha = 1.5$  (highly concentrated clusters with a rather flat mass function, see § 5.2). Our calculations indicate that at the present time some of these clusters have very small masses ( $\sim 1\%$  of the initial mass) but are rather highly concentrated (see Figs. 8 and 9).

The old open cluster Berkeley 17 is comparable to such a model with  $W_0 = 7$  and  $\alpha = 1.5$  of family 3. Berkeley 17 has an age of 10 Gyr to 13 Gyr, a distance to the Galactic center of  $R_g = 11$  kpc, a size of about  $\sim 5$  pc and a total mass in visible stars of about  $400 M_\odot$  (Phelps 1997). The model cluster experiences core collapse at  $t = 12$  Gyr, at which moment the total mass is only 1.3% of its initial value (see Table 3). At a distance of  $R_g = 11$  kpc from the Galactic center and with  $v_g = 220$  km/s, the initial mass of this model cluster would be  $M_0 \approx 2.3 \times 10^5 M_\odot$  (see Eq. [9]). At the moment of core collapse at  $t = 12$  Gyr,  $M \sim 3000 M_\odot$  and the half-mass radius is  $\sim 4$  pc. The majority of this mass is hidden in remnant stars, i.e.,  $\sim 900 M_\odot$  neutron stars and  $\sim 1700 M_\odot$  white dwarfs, and only  $\sim 400 M_\odot$  is in main-sequence stars. This cluster would be classified as a small and compact globular, or an old open cluster, according to the observed mass, integrated luminosity, and the age estimate. Just like Berkely 17.

Figure 12 shows the global mass function of this model at  $t = 12$  Gyr. The filled circles and the open circles represent the mass functions for the white dwarfs and for the main-sequence stars, respectively. The mass function for the main-sequence stars has the peak at  $m \sim 0.8 M_\odot$  and decreases with decreasing  $m$  after this peak. (The depletion of the main-sequence stars at  $m \sim 0.9 M_\odot$  is due to stellar evolution.) This shape of the mass function is the result of the preferential loss of low mass stars through the tidal boundary; high mass stars are more centrally concentrated than low mass stars due to mass segregation and therefore have less chance to escape. In general the global mass function becomes flatter as the cluster loses mass (e.g. Vesperini & Heggie 1997). However it is not so common to observe such inverted global mass functions as that shown in Fig. 12 in our surveyed samples. Such inverted mass functions appear only in long-lived remnant clusters, which have lost very large fractions ( $\sim 99\%$ ) of their initial masses over the two-body relaxation time scale. These remnant clusters were formerly the cores of more massive clusters where high mass stars were dominant as a result of mass segregation.

Interestingly De Marchi et al. (1999) observed an inverted mass function (actually, luminosity function)

---

<sup>2</sup>Note however, that  $c_{\text{King}}$  is not identical to the  $c$  (see § 5.2). However, the one- $\sigma$  error in the observed  $c_{\text{King}}$  is about 0.2 (Trager et al. 1993), which is larger than the difference in  $c_{\text{King}}$  and the  $c$  we used. Therefore we think that our results are robust.

with the peak at  $\sim 0.75M_{\odot}$ , which is similar to the mass function shown in Fig. 12, in the globular cluster NGC 6712. The luminosity function was measured at regions located between one and two times the half-light radius of the cluster. De Marchi et al. (1999) considered the inverted mass function as an evidence for severe tidal disruption. This interpretation is consistent with our findings discussed above. The local mass function at the half-mass radius for the model shown in Fig. 12 is similar to the global one, but decreases somewhat more rapidly with decreasing  $m$ . Our simulation results suggest that the initial mass of NGC 6712 might have been more than 100 times the present mass  $\sim 10^5M_{\odot}$  (Pryor & Meylan 1993).

#### 6.4. Effect of the tidal cut-off

To investigate the effect of the self-consistent tidal field compared with the adopted tidal cut-off, we performed some comparative  $N$ -body calculations. For this purpose we use the same initial conditions as for Figure 1. Each calculation is performed with a different implementation of the tidal field. For each implementation of the tidal-field we use exactly the same initial randomization of the masses, the positions and the velocities of all 1024 stars. The results are presented in Figure 13.

The solid line in Figure 13 represents the mean of ten computations with a tidal cut-off (model TCR1, the  $\sigma/2$  deviations are shown in Figure 1). The other lines represent the results for a self-consistent tidal field. For all models the same tidal force is used, but different cut-off radii are selected. (The cut-off radius is the radius where stars are removed from the calculations. For computational reasons it is convenient to set a cut-off radius even for calculations where a tidal field is used.) Stars in the models are removed as soon as they go beyond  $r_t$  (model TFR1; the T stands for tidal, F for field and the R stands for the radius, in units of the tidal radius, at which stars are removed from the simulation),  $2r_t$  (model TFR2),  $10r_t$  (model TFR10), and  $100r_t$  (model TFR100) from the cluster center. The mass given in Figure 13 is the mass contained in stars which are bound to the cluster.

The models presented in Figure 13 are indistinguishable for the first one billion years, where mass loss is dominated by stellar evolution. After that, model TCR1 and model TFR1 start to lose mass more rapidly than the other models. (This acceleration in mass loss is related to a too sudden removal of escaping stars which is caused by the small cut-off radius.) Model TFR1 keeps losing mass at a rate slightly higher than the other tidal field models. After about 2 Gyr the mass loss rate of model TCR1 becomes smaller than for the models with a tidal field. Not surprisingly, stars are removed more quickly if a tidal field is incorporated and if stars are removed closer to the tidal radius. Figure 13 shows that an artificial cut-off radius in excess of  $2r_t$  hardly affects the results in the models where a self consistent tidal field is incorporated.

Orbit-averaged Fokker-Planck methods (Cohn 1979, 1980) are based on the assumption that the time evolution of the gravitational potential is adiabatic, i.e., that the change in the potential occurs on a time scale much longer than the orbital periods of the stars in the cluster. The validity of this assumption becomes weaker as the number of stars decreases. In particular, when the mass loss due to stellar evolution is very violent, it can happen that the assumption is not valid anymore.

The Fokker-Planck model with 1K stars (see Figure 1) loses more mass in the first one billion years than the  $N$ -body models (TCR1, TFR1 to TFR100). This may be caused by the assumed adiabatic response of the Fokker-Planck models to changes in the potential. The cluster loses about 30% of its initial mass within 1 Gyr. Since the initial half-mass crossing time is about 0.5 Gyr, this potential change can hardly be called adiabatic, but impulsive instead. In spite of this breakdown of the assumption the Fokker-Planck models agree well with the  $N$ -body models (except model TFR1).

Models with a tidal cut-off behave in a similar fashion as the models with a self-consistent tidal field, if the cut-off radius is set big enough ( $\gtrsim 2r_t$ ). The difference between a rigid tidal cut-off and the more elaborate self-consistent tidal field are ill understood (see however Giersz & Heggie 1997), and we like to encourage further investigations.

## 7. Conclusions

We have investigated the evolution of star clusters including the effects of the steady tidal field of the parent galaxy and the mass loss from stellar evolution. TPZ demonstrated that excellent agreement between Fokker-Planck and  $N$ -body models is obtained, if *anisotropic* Fokker-Planck models are used in combination with *a new implementation* of the tidal field. These anisotropic Fokker-Planck models are considered more realistic than the isotropic models used by CW. The latter models show large deviations from the  $N$ -body calculations carried out by TPZ (see also Portegies Zwart et al. 1998). In this paper we have extended the study of TPZ to check agreement between anisotropic Fokker-Planck and  $N$ -body models for a much wider range of initial conditions.

The new implementation of the tidal boundary in our anisotropic Fokker-Planck models includes one free parameter  $\nu_{\text{esc}}$ . This parameter relates the time scale on which escapers are removed from the cluster relative to the dynamical time scale. We have found that a single value of  $\nu_{\text{esc}} = 2.5$  provides good agreement between  $N$ -body and Fokker-Planck calculations for a wide range of initial conditions. The introduction of the new boundary conditions allows us to perform Fokker-Planck calculations in a much wider range of parameter space, including varying the number of stars. This makes it possible to compare Fokker-Planck models directly with  $N$ -body models.

In the second part of this paper we carried out a survey of the evolution of globular clusters in the galaxy using our anisotropic Fokker-Planck models. The surveyed initial models are exactly the same as those chosen by CW. Our Fokker-Planck models live generally longer than the corresponding isotropic models of CW. The differences between our models and CW's are quite large in cases where CW concluded that the cluster dissolves without experiencing core collapse. The differences are smaller for clusters which start with a steep mass function and a high concentration and which reach core collapse before they dissolve (even in CW's calculations). These findings are consistent with the conclusions of the recent  $N$ -body calculations performed by Aarseth & Heggie (1998).

About half of the clusters calculated in our survey are disrupted before the current age of the Universe is reached. Most of the clusters that survive for a Hubble time experience core collapse at some time in the future. Only in four of our calculations core collapse occurs within 10 Gyr. Two of these clusters have lost more than 99% of their mass at the moment of core collapse. This possibly indicates that parameter space for core collapse within the age of the Universe is rather small.

We find a few clusters which are peculiar in the sense that they have very small masses ( $\sim 1\%$  of the initial mass) but are well concentrated at the present time. Such clusters may be observed as old open clusters, like Berkeley 17, rather than as small globular clusters. These clusters are peculiar at the present time also in the sense that they may have inverted global mass functions which decrease with decreasing stellar mass for  $m \lesssim 0.8M_\odot$ . A similar inverted mass function was observed in the globular cluster NGC 6712 by De Marchi et al. (1999) recently. Thus the mass function of NGC 6712 might indicate that the cluster has lost almost all ( $\gtrsim 99\%$ ) of the initial mass until the present time.

There seems to be some misunderstanding that clusters which have lost more than 50% of their initial mass are inevitably disrupted. This principle is based on the virial theorem and on the assumption of impulsive mass loss (Hills 1980). For the initial conditions of  $W_0 = 7$ ,  $\alpha = 1.5$ , and family 4, the first 50% mass of the cluster is lost within a few half-mass crossing times (see Fig. 5). Still, the cluster survives for several tens of billions of years to experience core collapse.

Comparison of the results of  $N$ -body calculations with various implementations of the galactic tidal field and cut-off boundary indicates that there may be a significant population of stars which are trapped outside the tidal radius of the cluster but are still bound to the stellar system.

We are grateful to Piet Hut, Junichiro Makino and Steve McMillan for many discussions and software development. We also thank Haldan Cohn, Douglas Heggie and Toshiyuki Fukushige for enlightening discussions. This work was supported in part by the Research for the Future Program of Japan Society for the Promotion of Science (JSPS-RFTP97P01102), and by NASA through Hubble Fellowship grant awarded by the Space Telescope Science Institute, which is operated by the Association of Universities for Research in Astronomy, Inc., for NASA under contract NAS 5-26555.

## REFERENCES

Aarseth, S., & Heggie, D. C. 1998, MNRAS, 297, 794

Binney, J., & Tremaine, S. 1987, Galactic Dynamics (Princeton University Press, Princeton)

Chernoff, D. F., & Weinberg, M. D. 1990, ApJ, 351, 121 (CW)

Chernoff, D. F. 1993, in Structure and Dynamics of Globular Clusters, ASP Conference Series Vol. 50, ed. S. G. Djorgovski & G. Meylan (San Francisco: ASP), p245

Cohn, H. 1979, ApJ, 234, 1036

Cohn, H. 1980, ApJ, 242, 765

De Marchi, G., Leibundgut, B., Paresce, F., & Pulone, L. 1999, A&A, 343, L9

De Marchi, G., & Paresce, F. 1995, A&A, 304, 202

De Marchi, G., & Paresce, F. 1995, A&A, 304, 211

Drukier, G. A., 1995, ApJS, 100, 347

Drukier, G. A., Cohn, H. N., Lugger, P. M., & Yong, H. 1999, accepted by ApJ

Fukushige, T., & Heggie, D. C. 1995, MNRAS, 276, 206

Giersz, M., & Heggie, D. C. 1994a, MNRAS, 268, 257

Giersz, M., & Heggie, D. C. 1994b, MNRAS, 270, 29

Giersz, M., & Heggie, D. C. 1997, MNRAS, 286, 709

Giersz, M., & Spurzem, R. 1994, MNRAS, 269, 241

Heggie, D. C., Ramamani, N., 1995, MNRAS 272, 317

Hills, J. G. 1980, ApJ, 225, 986

Hut, P. 1994, IAU 165, in Compact stars in binaries, eds. J. van Paradijs and E. P. J. van den Heuvel & E. Kuulkers, Kluwer, p. 377

Hut, P., Makino, J., & McMillan, S. 1995, ApJ, 443, 93

Janes, K. A., & Phelps, R. L. 1994, AJ, 108, 1773

King, I. 1966, AJ, 71, 64.

Kroupa, P. Tout, C. A., & Gilmore, G. 1990 MNRAS, 244, 76

Lee, H. M., & Ostriker, J. P. 1987, ApJ, 322, 123

Makino, J., & Aarseth, S. J. 1992, PASJ, 44, 141

Makino, J., Taiji, M., Ebisuzaki, T., & Sugimoto, D. 1997, ApJ, 480, 432

Makino, J. 1991, ApJ 369, 200

Marconi, G., Buonanno, R., Carretta, E., Ferraro, F. R., Fusi Pecci, F., Montegriffo, P., De Marchi, G., Paresce, F., & Laget, M. 1998, MNRAS, 293, 479

McMillan, S. L. W., 1986, ApJ 307, 126

McMillan, S. L. W., 1986, ApJ 306, 552

McMillan, S. L. W., Hut, P. 1996 ApJ 467, 348

Meylan, G., & Heggie, D. C., 1997, A&A Rev. 8,1

Phelps, R. L. 1997, ApJ, 483, 826

Portegies Zwart, S. F., & Verbunt, F. 1996, A&A, 309 179

Portegies Zwart, S. F., & Yungelson, L. 1998, A&A, 332, 173

Portegies Zwart, S. F., Tout, Ch., & Lee, H. M. 1998a, in Highlights of Astronomy, Vol. 11, ed. J. Andersen, in press (astro-ph/9710209)

Portegies Zwart, S. F., Hut, P., Makino, J., & McMillan, S. L. W. 1998b, A&A, 337, 363

Pryor, C., & Meylan, G. 1993, in Structure and Dynamics of Globular Clusters, ASP Conference Series Vol. 50, ed. S. G. Djorgovski & G. Meylan (San Francisco: ASP), p357

Ross, D. J., Mennim, A., & Heggie, D. C. 1997, MNRAS, 284, 811

Scalo, J. M. 1986, Fund. of Cosm. Phys., 11, 1

Spitzer, L. Jr. 1987, Dynamical Evolution of Globular Clusters (Princeton University Press, Princeton)

Spurzem, R., & Takahashi, K. 1995, MNRAS, 272, 772

Takahashi, K. 1995, PASJ, 47, 561

Takahashi, K. 1996, PASJ, 48, 691

Takahashi, K. 1997, PASJ, 49, 547

Takahashi, K., Lee, H. M., & Inagaki, S. 1997, MNRAS, 292, 331

Takahashi, K., & Portegies Zwart, S. F. 1998, ApJ, 503, L49 (TPZ)

Trager, S. C., Djorgovski, S., & King, I. R. 1993, in Structure and Dynamics of Globular Clusters, ASP Conference Series Vol. 50, ed. S. G. Djorgovski & G. Meylan (San Francisco: ASP), p347

Table 1. Stellar evolution models.

$m_{\text{ini}}/M_{\odot}$	$\log(t_{\text{MS}}/\text{yr})$		$m_{\text{fin}}/M_{\odot}$	
	CW	SeBa	CW	SeBa
0.40	11.3	11.3	0.40	0.40
0.60	10.7	10.8	0.49	0.52
0.80	10.2	10.4	0.54	0.56
1.00	9.89	10.0	0.58	0.59
2.00	8.80	9.02	0.80	0.69
4.00	7.95	8.29	1.24	0.80
8.00	7.34	7.64	0.00	1.33
15.00	6.93	7.14	1.40	1.34

Table 2. Families.

Family	$F$	$t_{\text{rlx}}/\text{Gyr}$	$t_{\text{rh}}/\text{Gyr}$
1	$5.00 \times 10^4$	128	2.4
2	$1.32 \times 10^5$	339	6.4
3	$2.25 \times 10^5$	577	11.0
4	$5.93 \times 10^5$	1522	29.0

<sup>a</sup>The half-mass relaxation time  $t_{\text{rh}}$  is calculated for  $W_{\odot} = 3$  and  $\bar{m} = 1M_{\odot}$ .

Table 3. Survey results.

$W_0$	$\alpha$	Family							
		1		2		3		4	
		CW	Aa	CW	Aa	CW	Aa	CW	Aa
1	1.5	D	D	D	D	D	D	D	D
		$9.2 \times 10^{-3}$	0.017	$9.4 \times 10^{-3}$	0.018	$9.3 \times 10^{-3}$	0.018	$9.3 \times 10^{-3}$	0.018
		0.78	0.61	0.78	0.63	0.78	0.63	0.79	0.62
	2.5	D	D	D	D	D	D	D	D
		0.034	0.31	0.034	0.32	0.035	0.32	0.034	0.33
		0.77	0.55	0.77	0.56	0.76	0.56	0.77	0.57
	3.5	D	C	D	D	D	D	D	D
		2.5	22	2.9	24	3.1	28	3.2	36
		0.64	0.021	0.73	0.27	0.74	0.34	0.76	0.44
3	1.5	D	D	D	D	D	D	D	D
		0.014	0.026	0.014	0.026	0.014	0.026	0.014	0.026
		0.53	0.42	0.55	0.41	0.55	0.41	0.54	0.41
	2.5	D	D	D	D	D	D	D	D
		0.28	2.2	0.29	2.7	0.29	2.9	0.29	3.0
		0.46	0.27	0.47	0.32	0.48	0.34	0.49	0.37
	3.5	C	C	C	C	D	C	D	C
		21.5	32	44.4	80	42.3	129	43.5	313
		0.078	0.17	0.035	0.14	0.085	0.13	0.28	0.11
7	1.5	D	C	D	C	D	C	D	C
		1.0	3.1	3.0	7.7	4.2	12	5.9	27
		0.022	0.010	$3.3 \times 10^{-3}$	0.012	$8.0 \times 10^{-3}$	0.013	0.023	0.011
	2.5	C	C	C	C	C	C	C	C
		9.6	10	22.5	24	35.5	38	83.1	89
		0.26	0.32	0.26	0.32	0.26	0.32	0.25	0.31
	3.5	C	C	C	C	C	C	C	C
		10.5	9.9	31.1	31	51.3	53	131.3	135
		0.57	0.65	0.51	0.58	0.48	0.55	0.49	0.55

<sup>a</sup> The results of Chernoff & Weinberg (1990, CW) are taken from their Table 5. Aa represents our results for the anisotropic Fokker-Planck models with the apocenter criterion.

<sup>b</sup> The first entry describes the fate of the cluster at the end time of the simulation  $t_{\text{end}}$ : C (core collapse) or D (disruption). The second entry is  $t_{\text{end}}$  in units of  $10^9$  yr. The third entry is the cluster mass at  $t_{\text{end}}$  in units of the initial mass.

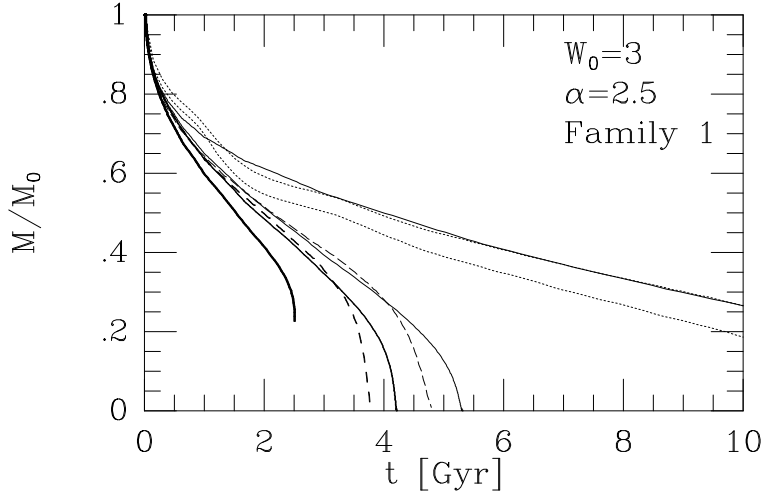


Fig. 1.— Comparison between Aa Fokker-Planck models (solid lines) and  $N$ -body models (dotted and dashed lines) for the mass evolution. The initial conditions are given by  $W_0 = 3$ ,  $\alpha = 2.5$ , family 1. The thickest solid line represents the Fokker-Planck model with the instantaneous escape condition, which corresponds to the the limit of  $N \rightarrow \infty$ . The three subsequent solid lines are models for 32K (thick), 16K, and 1K stars, respectively, with  $\nu_{\text{esc}} = 2.5$ . The left and right dashed lines give the results of the  $N$ -body simulations for 32K (thick) and 16K stars, respectively. The two dotted lines represent the  $\frac{1}{2}\sigma$  deviation from the mean of the 10 performed runs with 1K stars.

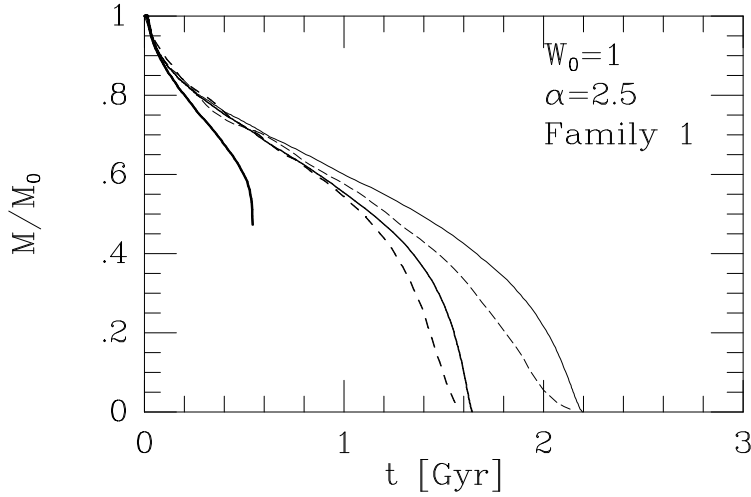


Fig. 2.— Comparison between Aa Fokker-Planck (solid) and  $N$ -body (dotted) models for the mass evolution. The initial conditions are given by  $W_0 = 1$ ,  $\alpha = 2.5$ , family 1, and  $N=8K, 16K$ . The thickest solid line represents the Fokker-Planck model with the instantaneous escape condition, which corresponds to the the limit of  $N \rightarrow \infty$ . The other Fokker-Planck models ( $N=8K, 16K$ ) are calculated using  $\nu_{\text{esc}} = 2.5$ . Thickness of the lines stand for largeness of  $N$ .

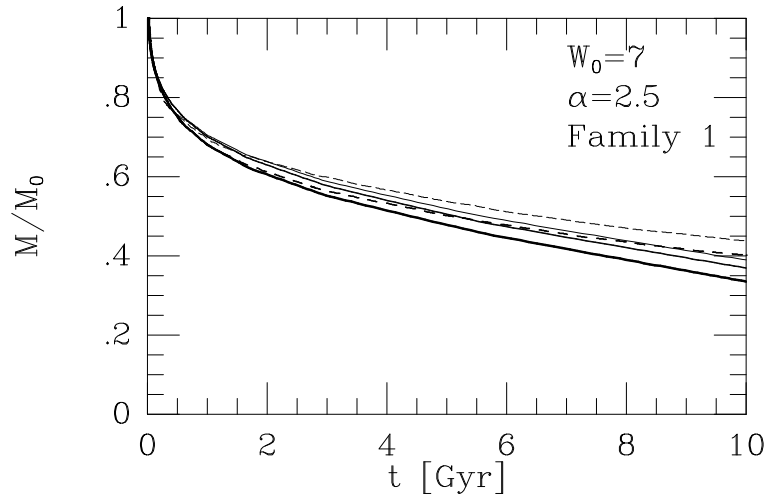


Fig. 3.— The same as Fig. 2, but the initial conditions are given by  $W_0 = 7$ ,  $\alpha = 2.5$ , family 1, and  $N=4K$ ,  $8K$ , or  $\infty$  (the Fokker-Planck model only).

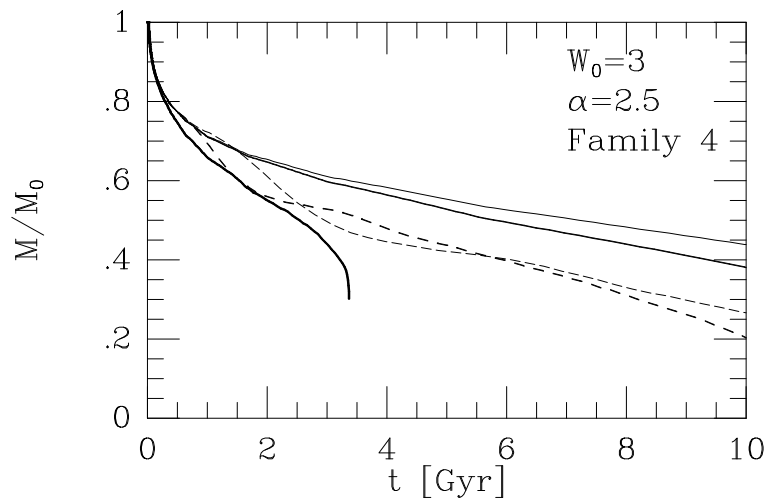


Fig. 4.— The same as Fig. 2, but the initial conditions are  $W_0 = 3$ ,  $\alpha = 2.5$ , family 4, and  $N=8K$ ,  $16K$ , or  $\infty$  (the Fokker-Planck model only).

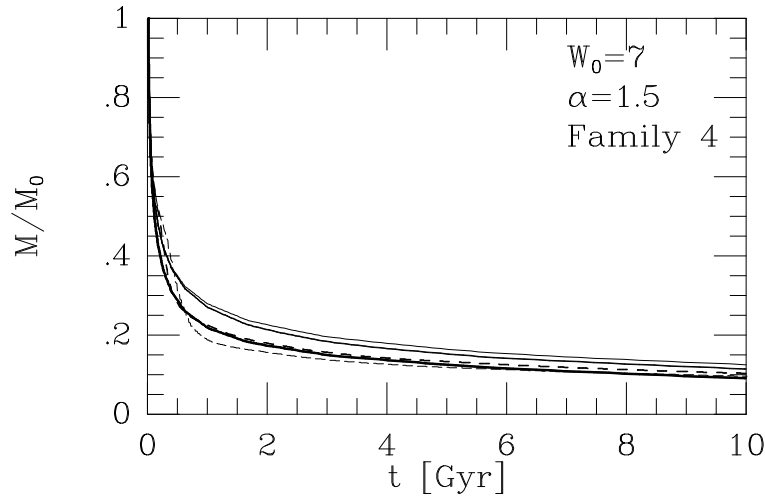


Fig. 5.— The same as Fig. 2, but the initial conditions are given by  $W_0 = 7$ ,  $\alpha = 1.5$ , family 4, and  $N=8K$ ,  $16K$ , or  $\infty$  (the Fokker-Planck model only).

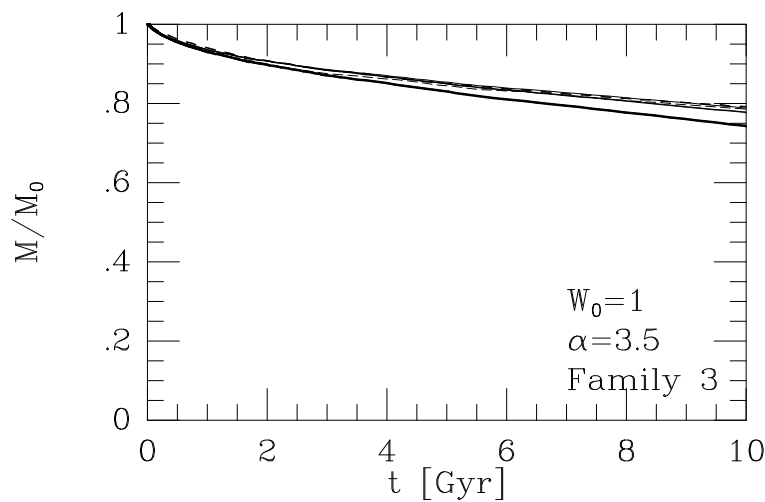


Fig. 6.— The same as Fig. 2, but the initial conditions are given by  $W_0 = 1$ ,  $\alpha = 3.5$ , family 3, and  $N=8K$ ,  $16K$ , or  $\infty$  (the Fokker-Planck model only).

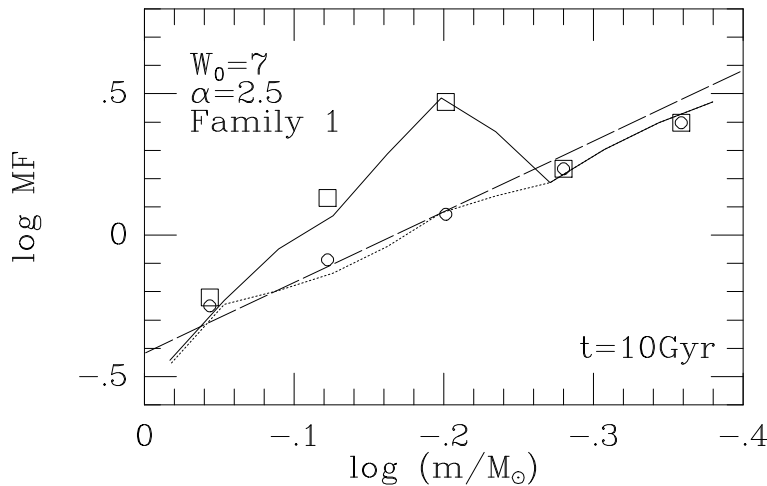


Fig. 7.— The global mass function for the model with the initial conditions of  $W_0 = 7$  and  $\alpha = 2.5$  from family 1 at  $t = 10$  Gyr. The dashed line gives the initial mass function. The mass functions are normalized at each epoch. The mass functions for the Fokker-Planck model are given by symbols, and the  $N$ -body results are given by lines. The squares give the mass function for all the stars and the circles give the mass function for the main-sequence stars alone. The  $N$ -body results are also divided in the same categories (upper line for all the stars and dotted line for the main-sequence stars).

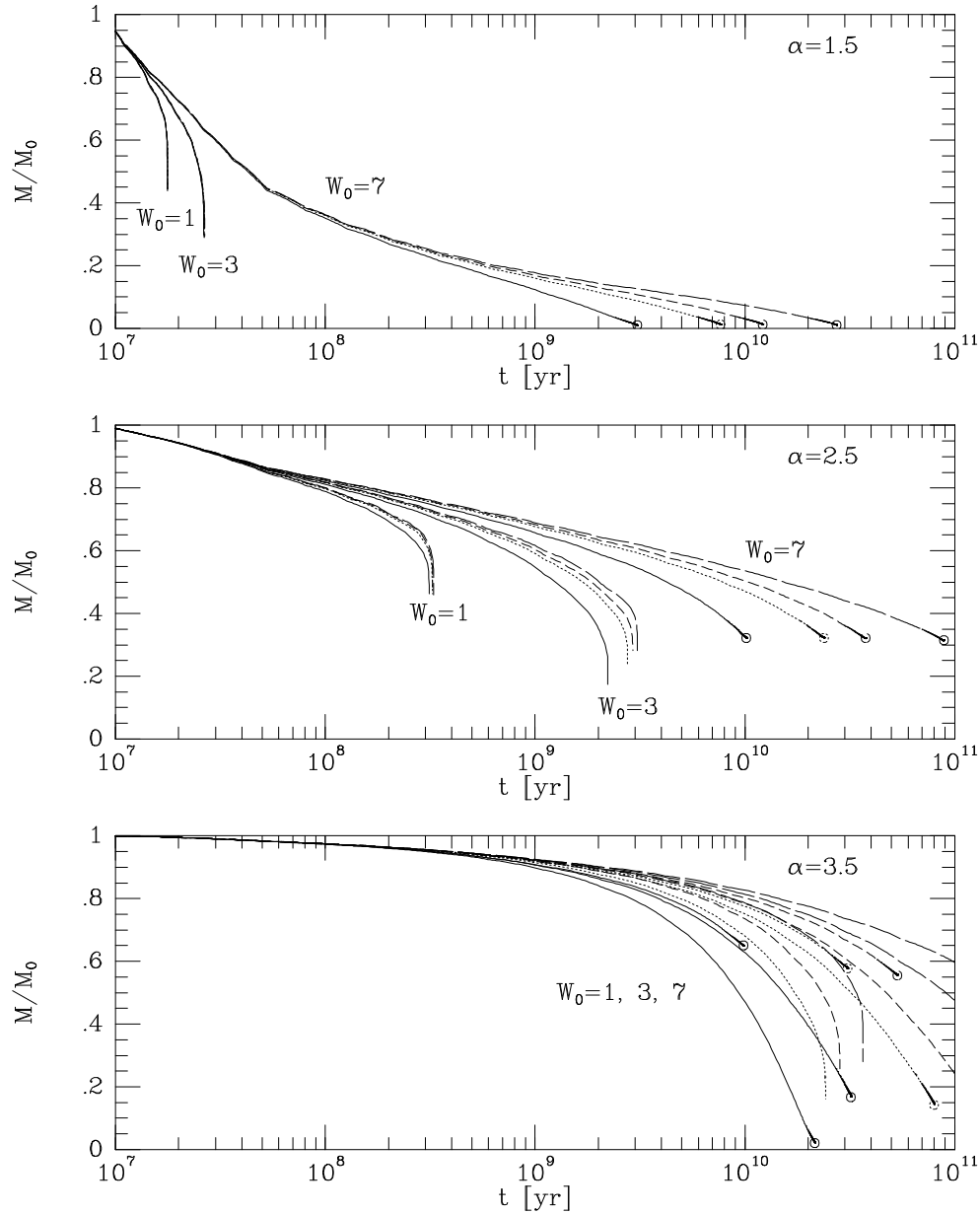


Fig. 8.— Results of the Fokker-Planck survey simulations: Evolution of the total mass. Three panels from top to bottom show results for the initial mass functions of  $\alpha=1.5$ , 2.5, and 3.5. Families 1 to 4 are plotted with solid, dotted, short dashed, and long dashed lines, respectively. The circles at the end points of some lines indicate that those simulations stop at the time of core collapse.

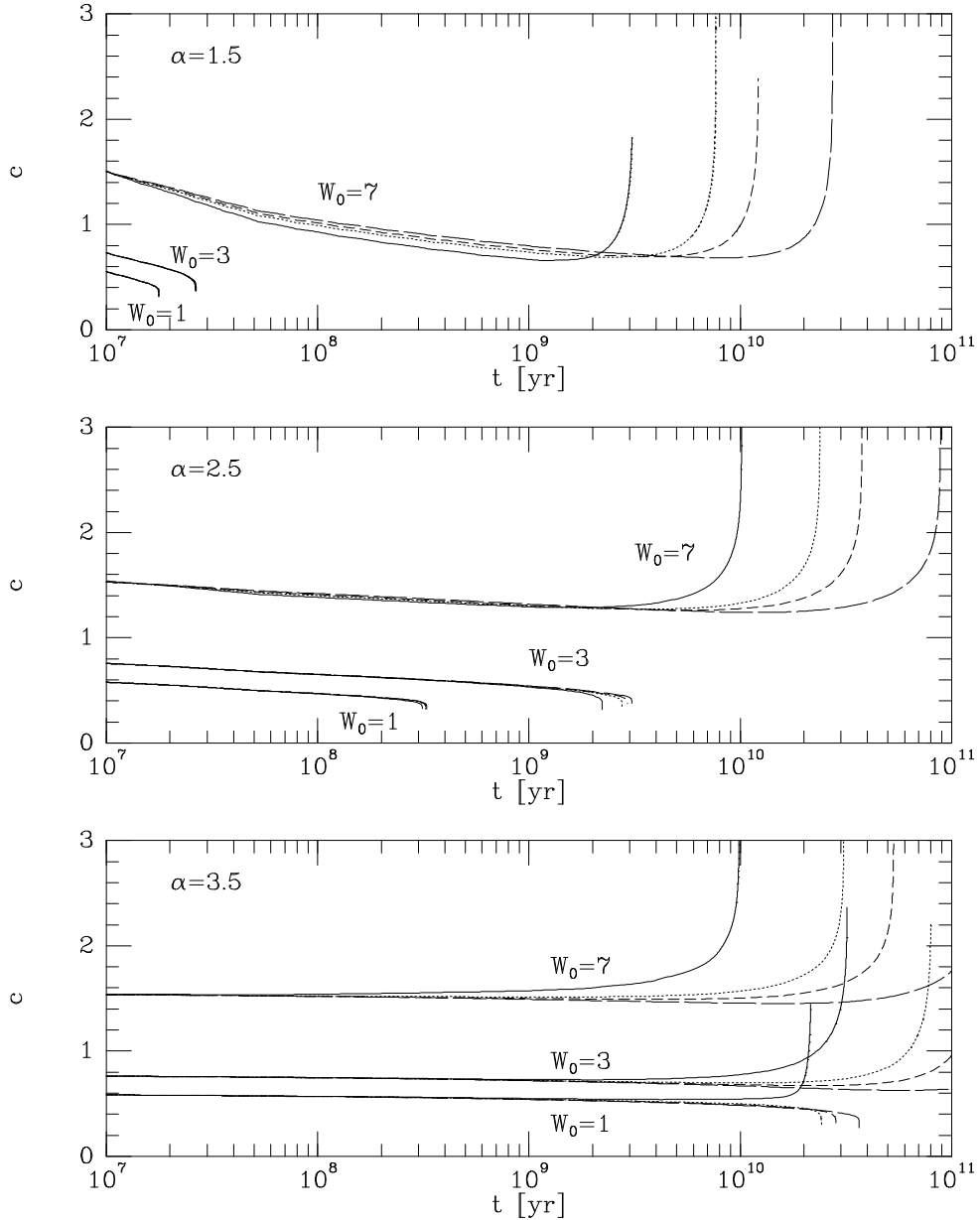


Fig. 9.— Results of the Fokker-Planck survey simulations: Evolution of the concentration  $c$ . The notation in this figure is the same as that in Fig. 8.

*Family 1*

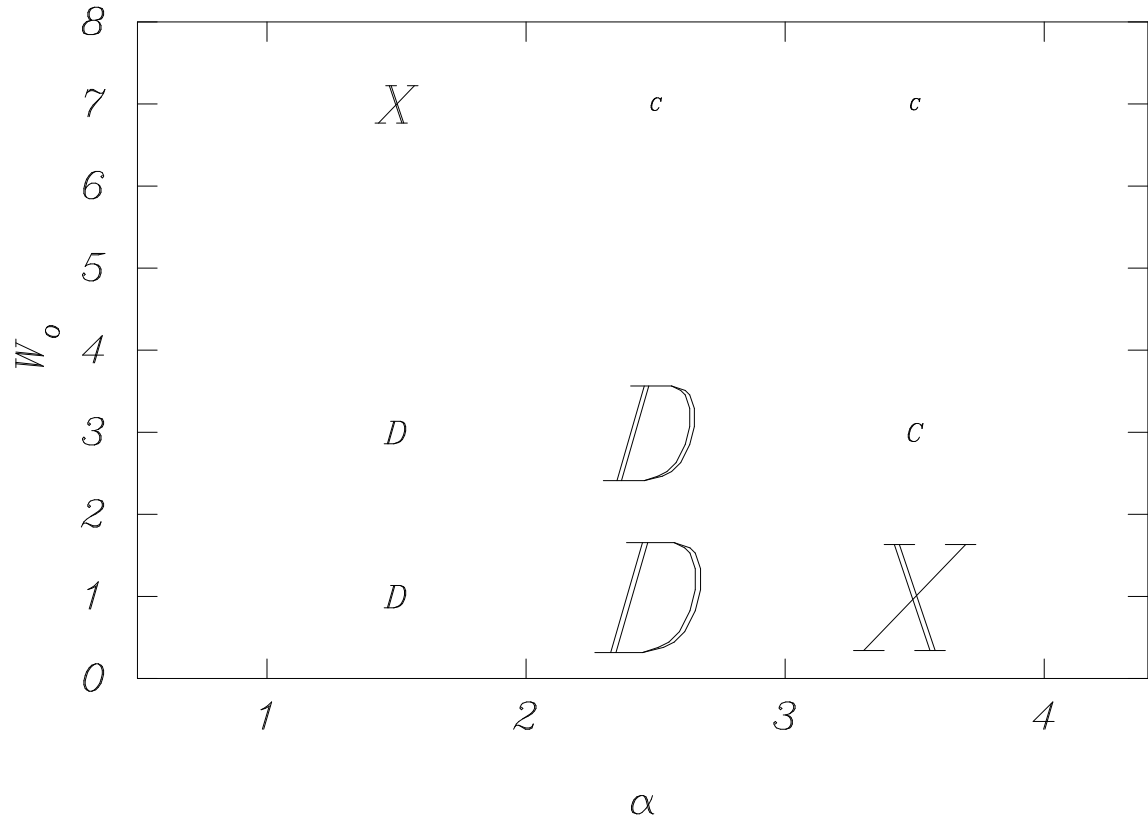


Fig. 10.— Graphical representation of the difference between the Aa models and the CW models in the survey results (see Tab 3) for family 1. The power-law index  $\alpha$  of the initial mass function is given along the X-axis and the initial value for  $W_0$  is given along the Y-axis. The symbols  $C$  and  $D$  indicate the end states of the simulations, collapse or disruption, respectively. An  $X$  indicates that the result of CW is disruption where we arrive at a collapsing cluster. The size of the letters is proportional to the lifetime at which we arrive as fraction of the lifetime of the cluster calculated by CW; a larger symbol indicates a larger discrepancy.

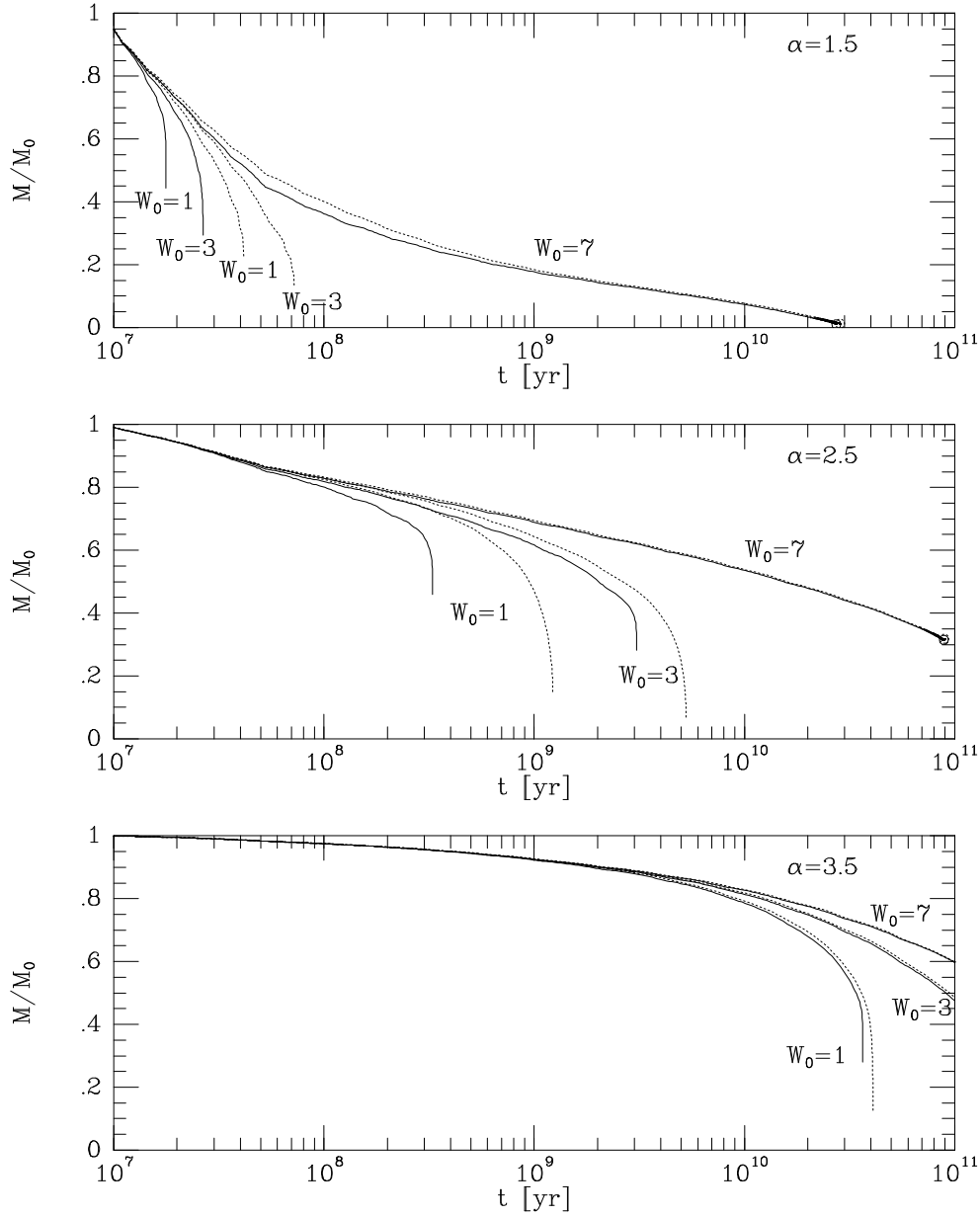


Fig. 11.— Comparison of the mass evolution between the models of  $N = 3 \times 10^5$  clusters (dotted lines) and the models of  $N \rightarrow \infty$  clusters (solid lines, the models shown in Fig. 8). Only the models of family 4 are shown. Three panels from top to bottom show results for the initial mass functions of  $\alpha=1.5$ , 2.5, and 3.5.

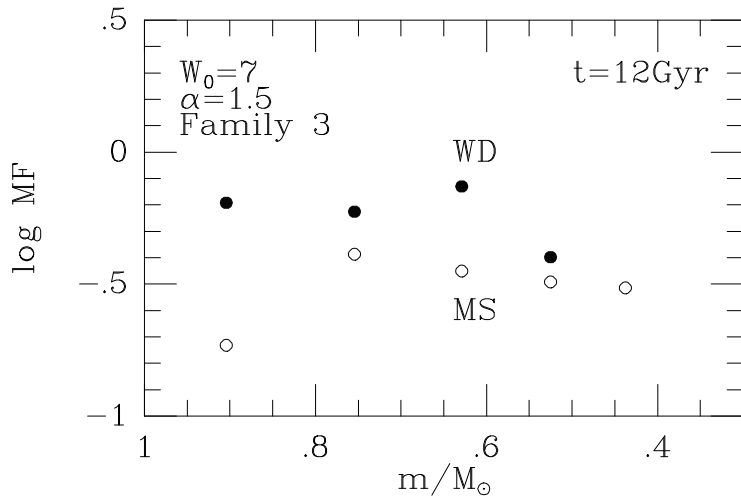


Fig. 12.— The global mass function for the model with the initial conditions of  $W_0 = 7$ ,  $\alpha = 1.5$ , and family 3, from the Fokker-Planck survey, at  $t = 12$  Gyr. The open circles represent the mass function of the main-sequence stars, and the filled circles represent that of the white dwarfs.

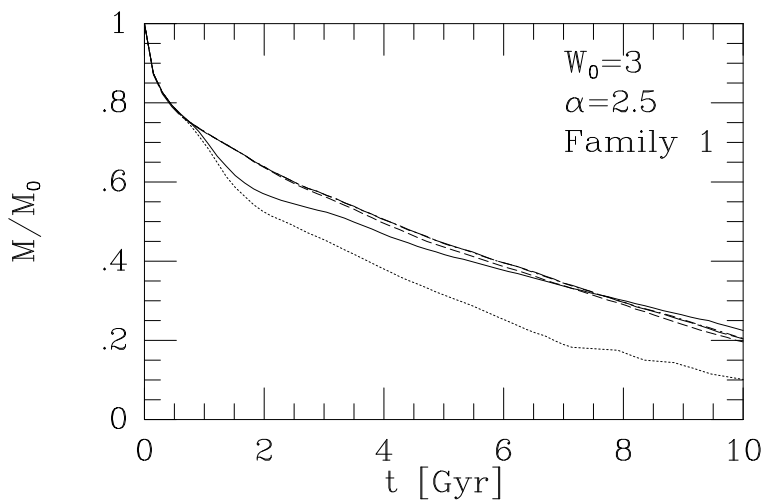


Fig. 13.— Mass as a function of time for various  $N$ -body models with 1K stars (for  $\alpha = 2.5$ ,  $W_0 = 3$ , and family 1) for different implementations of the tidal field. Each line represents the mean of ten calculations. The solid line is calculated with a simple tidal cut-off as is used for all other  $N$ -body calculations in this paper. The other lines give the results of calculations with a self-consistent tidal field in which stars are removed beyond the radii  $r_t$  (dotted),  $2r_t$  (short dashed),  $10r_t$  (long dashed), and  $100r_t$  (dash-dotted). The last two lines are almost indistinguishable.